RESEARCH OF POLARIZATION PROPERTIES OF THE BIREFRINGENT WAVEGUIDES COUPLING POINT AT DIFFERENT POLISH ANGLES

V A Shulepov, S M Aksarin.
Saint-Petersburg National Research University of Informational Technologies, Mechanics and Optics, Saint-Petersburg, Russia

E-mail: shulepov_vladimir@mail.ru

Abstract. Integrated optical birefringent waveguides are widely used in the field of phase interferometric fiber optic sensors. In sensors integrated optical waveguides are coupled to birefringent fiber waveguides. Due to different optical properties polarization conversion occurs at waveguides coupling point which may cause parasite interference to the signal of fiber optic sensors.

1. Introduction

Fiber optic sensors (FOS) are widely used in many high-tech sectors due to their resistance to electromagnetic disturbances, possession of small weight and size parameters and relatively low cost [1]. Phase interferometric detectors (PID) are considered to belong to the most accurate ones. Among FOS a fiber optic gyro (FOG), which is based on the Sagnac interferometer [2], is recognizable. FOG is an essential instrument for naval and aircraft navigation, as well as for spacecraft orientation and stabilization. Multifunctional integrated optical scheme (MIOS) is one of the FOG's elements. It is an integrated-optical scheme comprised of channel waveguides with the X-shaped coupler topology fabricated on lithium niobate crystal, fabricated by diffusion of titanium. The advantage of the presented lithium niobate crystal is that is enables the modulation of birefringence with high efficiency, and low optical loss (about 3.5 dB), as well as coupling to a single mode fiber.

At the FOG design stage the fiber with high birefringence must be used to achieve the maximum visibility of the signal interference pattern, to improve the device accuracy and reduce the phase interferometric noise.Also, the complexity of the optical interconnection of an integrated optical waveguide to an optical birefringent fiber, since it is necessary to connect all the birefringent elements of the optical scheme with high precision matching axes [2,3]. Since the refractive indices of the integral optical waveguide and fiber lightguide are different, the back reflection occurs crystal boundary under the Fresnel's law [4]. It is partially compensated by tilting ends of the crystal by 10° [3]. Due to that the back reflection occurring on the boundary of the crystal, are partially output to the substrate but not completely.

Therefore, to avoid the parasite interference between the reflected wave trains, the waveguides are deliberately fabricated with different lengths greater than the coherence

length of the source. The MIOS features described above are achieved due to the fact that the straight sections of the channel waveguides are positioned at the 3˚ angle to the optical axis of the crystal, which is displayed in Fig. 1**.**

Due to the refractive index differences of the fiber and crystal and its facet tilt, from the Snell's law[5], the differences between the optimal tilt angles of the fiber and crystal appear. Which are respectively shown below:

10,5˚ – 7 ˚;

19,5˚ – 13 ˚.

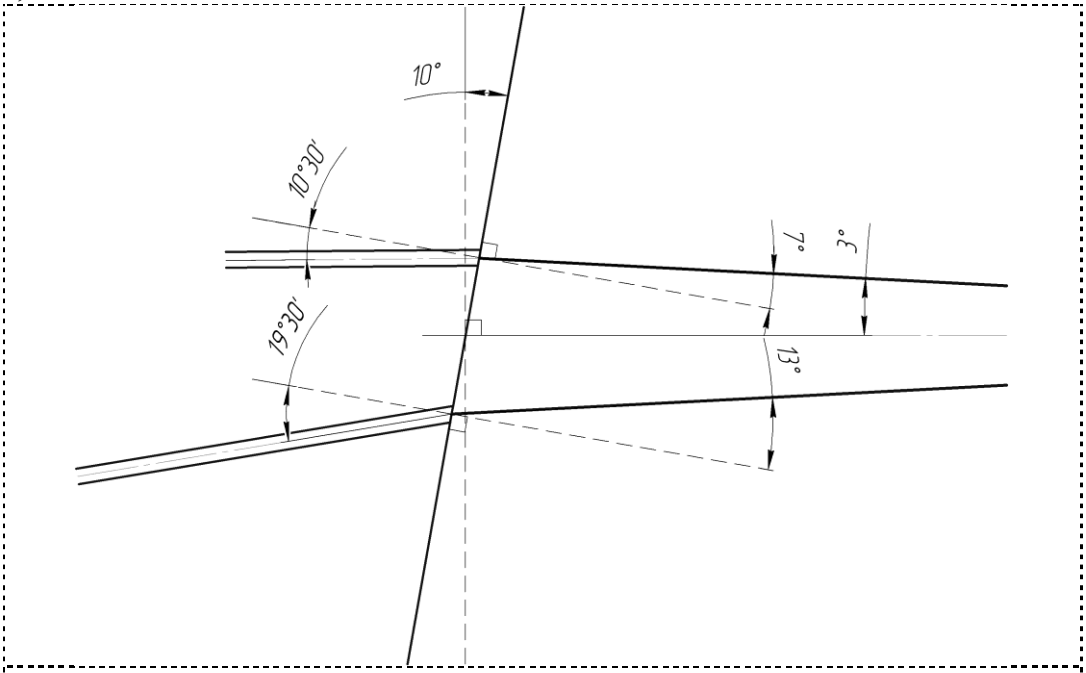

Fig. 1. The schematic figure of the MIOS to fiber coupling angles.

2. The optical scheme

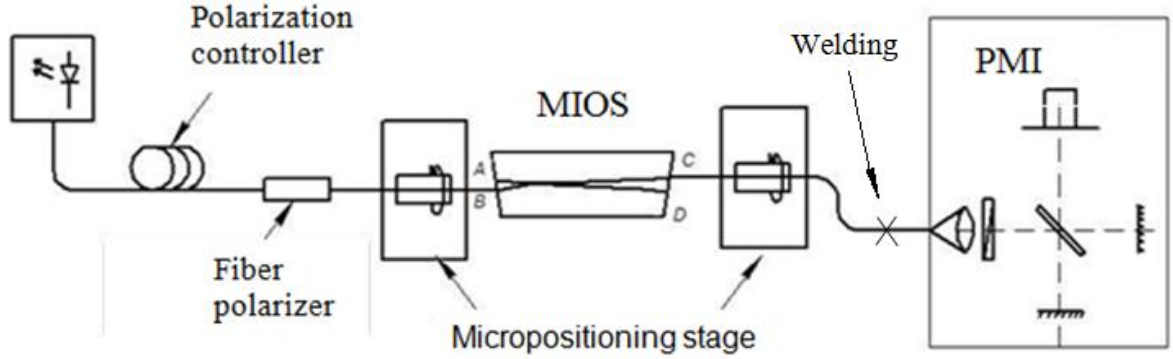

Fig. 2. The optical scheme for measuring of the conversion of the polarization state of the optical radiation.

To carry out this investigation the setup had been assembled. It consists of a light source, polarization controller, MIOS, single-mode fiber for MIOS optical radiation input/output and the polarization Michelson interferometer. The optical radiation from the source was coupled through the polarization controller through one of the MIOS ports; on the MIOS input there is the polarizer which is transmissive to one of the orthogonal components. Further, in one of the opposite ports the radiation was received with the fiber, polished at an angle 19,5˚, 10,5˚ and 0˚. After that, the optical radiation was coupled into the polarization Michelson interferometer. With the help of which, the visibility analysis had been carried out at a different displacement of one of interferometer arms, based on which the value of the coupling point polarization conversion was found.

3. The research

To avoid the of parasite interference peaks influence on the measurement results the graph of the interference pattern visibility distribution dependence on the interferometer arm displacement was obtained which is shown in Fig.1.

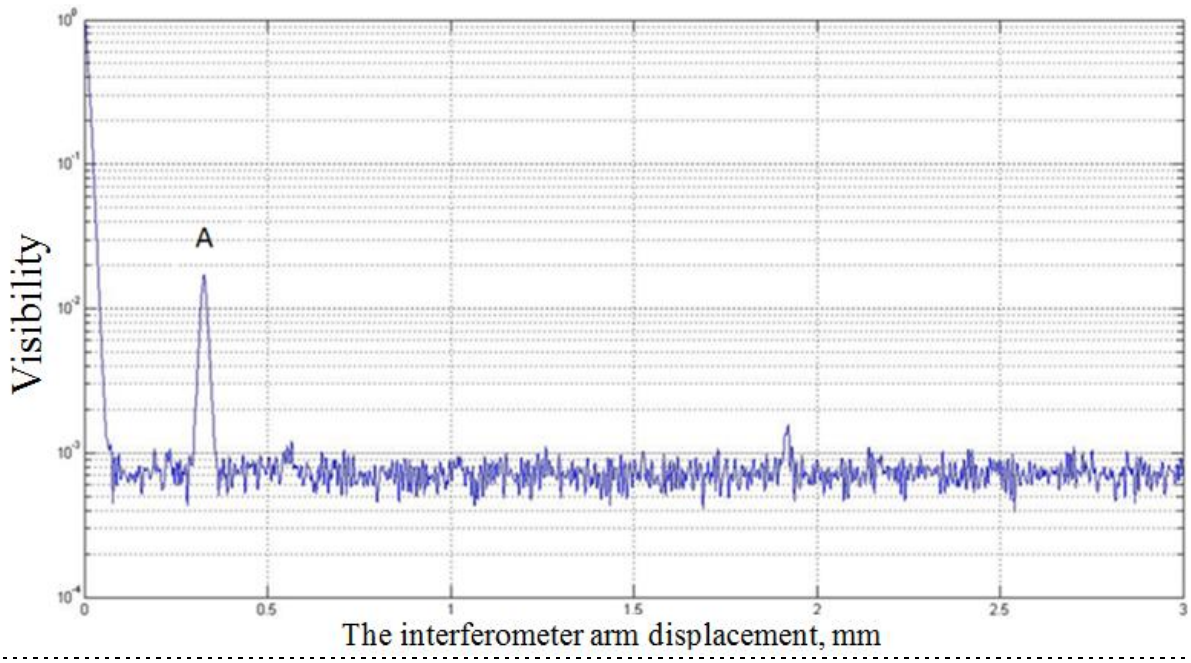

Fig. 3. The interference pattern visibility distribution dependence on the interferometer arm displacement after the light from the source passes though the polarization controller.

In fig. 3 point A - parasite interferometer peak from the radiation source.

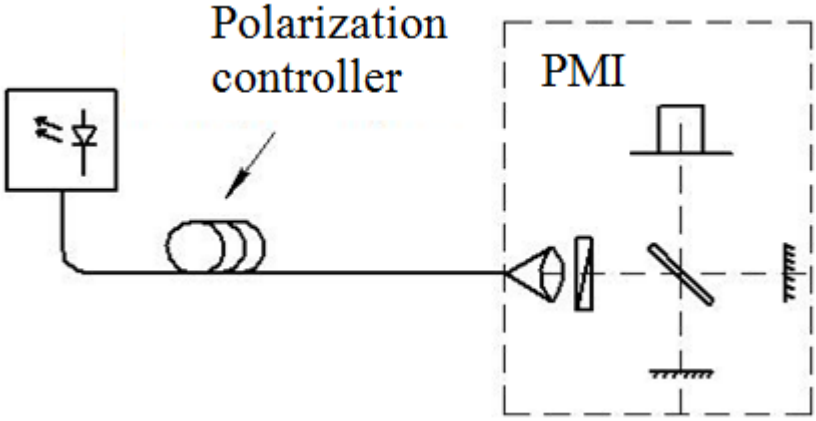

Fig. 4. Scheme, designed to eliminate the influence of parasitic interferometer peaks. PMI – polarization Michelson interferometer.

Further, the graphs of the interference pattern visibility distribution dependence on the interferometer arm displacement after the light from the source passes though the polarization controller were obtained to take measurements (Fig. 2). For the fibers with different tilt angles the extinction ratio value was measured at the coupling points with the formula (1).

$$ER = \frac{4 \cdot V_c^2}{\left(\sqrt{1 - 4 \cdot V_c^2} + 1\right)} \qquad (1)$$

Where V_c - the value of the interference pattern visibility at the coupling point.
The example of scanning is shown below.

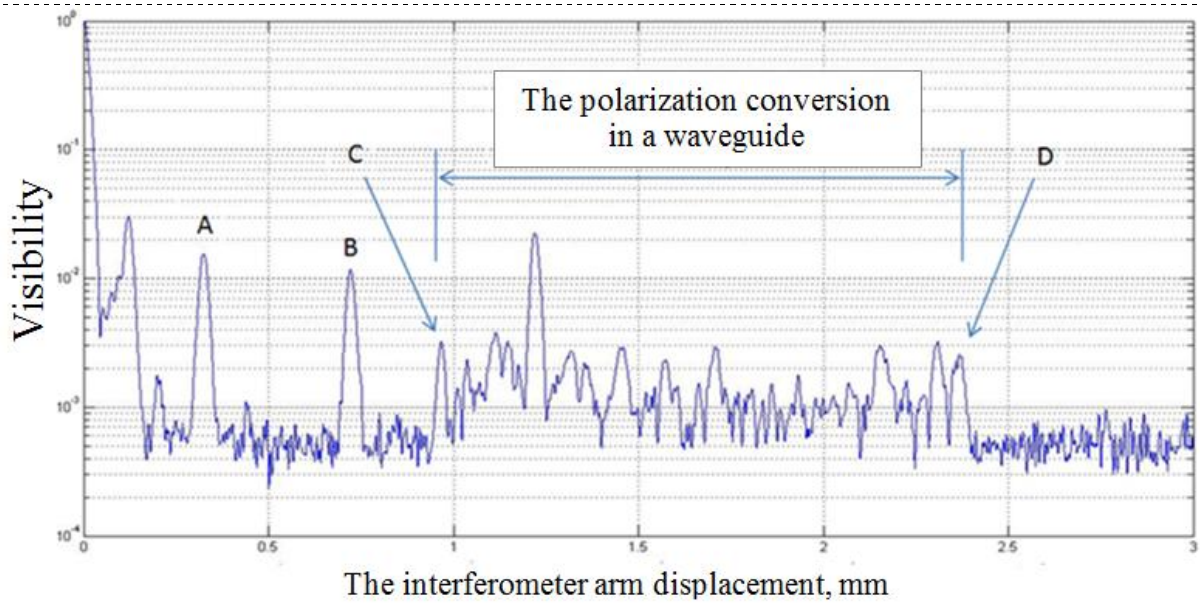

Fig. 5. The interference pattern visibility distribution dependence on the interferometer arm displacement after the light passes through the scheme used in the research.

A - parasite interferometer peak from the radiation source.
B - the conversion of the polarization state in the welding point of optical fibers.
C – the investigated coupling point of waveguide with fiber.
Segment CD – the polarization conversion in a waveguide.

The research results are presented in the table below:
Table 1. The extinction ratio at the coupling point of the fiber with the waveguide at various tilt angles of end polishing.

	Tilt angle of the waveguide	**Tilt angle of end polishing**	**The extinction ratio at the coupling point of the fiber and the waveguide, dB**
With immersion	13˚	0˚	-45,8
		19,5˚	-57,1
Without immersion	13˚	0˚	-45,2
		19,5˚	-50,5
With immersion	7˚	0˚	-46,2
		10,5˚	-45,8
Without immersion	7˚	0˚	-39,8
		10,5˚	-48,4

4. Conclusion

From the results presented in the table we can make a conclusion that the extinction ratio value degrades at the deviation from the optimum tilt angle at which the maximum radiation coupling efficiency is observed. Also, the coupling point extinction ratio with immersion it better than without it.

Acknowledgements

This work was done in ITMO University and was supported by the Ministry of Education and Science of the Russian Federation under the project 02.G25.31.0044.

References

[1] Okosi T, Okamoto K, Otsu M, Nisihara H, Kauma K and Hatate K, Fiber Optic Sensors, Leningrad: Energosamizdat, 1991. p. 256

[2] Lefevre H. The Fiber-Optic Gyroscope. London: Artech House, 1992. p. 313

[3] Аксарин С.М. *Исследование поляризационных методов и технологии согласования волоконно-оптических и интегрально-оптических волноводов*. Диссертация на соискание ученой степени к.ф.-м.н., СПб., (2014).

[4] Сивухин Д.В. *Общий курс физики. Том IV. Оптика*. Москва: "ФИЗМАТЛИТ", с. 792, (2005).

[5] Детлаф А.А., Яворский Б.М. *Курс физики. Том 3. Волновые процессы. Оптика. Атомная и ядерная физика*. Москва: "Высшая школа", с. 511, (1979).